Bull. Mater. Sci. (2019) 42:11
https://doi.org/10.1007/s12034-018-1726-8

Impact of sulphurization environment on formation of Cu_2ZnSnS_4 films using electron beam evaporated stacked metallic precursors

P K KANNAN, SUSHMITA CHAUDHARI and SUHASH R DEY*
Department of Materials Science and Metallurgical Engineering, Indian Institute of Technology Hyderabad, Kandi, Sangareddy 502285, India
*Author for correspondence (suhash@iith.ac.in)

MS received 2 February 2018; accepted 10 May 2018; published online 17 January 2019

Abstract. The superiority of copper zinc tin sulphide (Cu_2ZnSnS_4; CZTS) over the existing absorber layer materials is inevitable owing to its cheap, non-toxic and earth abundant constituents with high absorption coefficient value. In the present study, CZTS films are prepared by sulphurizing electron beam deposited precursors of glass/Cu/Zn/Sn/Cu and glass/Cu/Sn/Zn/Cu stacking sequences in two different environments i.e., elemental S powder and 5% $H_2S + N_2$ gas at different ramping rates. The effect of sulphurization environment and sulphurization ramping rate on the formation of CZTS is investigated using X-ray diffraction and Raman spectroscopy. The morphology and composition of the films are analysed respectively using field emission gun scanning electron microscopy and energy dispersive X-ray spectroscopy. It is observed that films prepared in elemental S powder at a low ramping rate exhibit better crystallinity with less impurity phases. The presence of ZnS is observed in all the films, while the presence of SnS is observed in films prepared with H_2S gas alone, thus concluding that sulphurization in the presence of elemental S powder at a low ramping rate is highly favourable for CZTS film formation. CZTS films with minor ZnS impurity with a bandgap of 1.48 eV is successfully fabricated by using a glass/Cu/Zn/Sn/Cu precursor stack.

Keywords. Electron beam evaporation; ramping rate; CZTS.

1. Introduction

Copper zinc tin sulphide (Cu_2ZnSnS_4; CZTS) is one of the effective photon absorber layers used in inorganic solar photovoltaics. It has an optimum direct bandgap of 1.45 eV with a high absorption coefficient of 10^4 cm^{-1} and is entirely constituted with earth abundant and non-toxic elements, which makes it suitable as a potential alternative for already commercialized $CuIn_xGa_{1-x}Se_2$ (CIGS) [1,2]. Despite all the advantages over CIGS, the maximum experimental efficiency achieved by CZTS solar cell is only 13.8% which is very low compared to the efficiency achieved with CIGS [3,4]. Due to its quaternary constituents, formation of binary and ternary sulphide secondary phases is a major concern while synthesizing CZTS thin films. Hence, understanding the growth processes under different sulphurization conditions is highly crucial in minimizing the formation of secondary phases [5]. Precedent literature reveals that non-stoichiometric Zn rich Cu poor CZTS films yield maximum efficiency [6]. Hence, the probability of formation of secondary phases increases at this preferred non-stoichiometric condition which further narrows down the phase pure CZTS formation region in its ternary phase diagram [1].

CZTS films can be prepared by vacuum-based methods like electron beam evaporation [7], sputtering [8] etc., and non-vacuum techniques like dip coating [9,10], spin coating [11], electrodeposition [12] etc. Among the vacuum-based techniques, CZTS films can be prepared by (i) sulphurization of the metallic precursors deposited sequentially [13–15], (ii) deposition of metallic sulphide precursor films and annealing in an inert environment [16,17] and (iii) deposition using a quaternary CZTS target [5,18,19].

Su *et al* [15] fabricated CZTS films through sequential electrodeposition of metallic precursors and observed that the compositional ratio and stacking order have a major role in CZTS phase formation and they successfully prepared a 93% phase pure CZTS film with a glass/Zn/Sn/Cu precursor stack. Recent studies from Thota *et al* [20] and Olgar *et al* [21] also reveal that films having a Cu layer adjacent to both Sn and Zn layers have enhanced performance as an absorber layer due to the uniform diffusion of the precursor layers while annealing. Also, Thota *et al* [20] studied the effect of all the three constituent metallic layers as the capping layer and found that films with Cu at the top of stacking have enhanced electrical characteristics due to the minimal loss of volatile Sn and Zn from the precursor. Kim and Yoo [13] also concluded that films prepared with Cu at the top have enhanced grain sizes which may lead to superior performance.

In the case of CZTS films prepared through sequential deposition of metallic precursors, sulphurization of the films can be done either in the presence of elemental S powder or H_2S gas [5,14,15,22]. By optimizing the precursor stacking

sequence, sulphurization ramping rate and environment, formation of impurity phases can be reduced effectively. Hence, in this study, the variation in ramping rate and sulphurization environment on the CZTS formation is investigated for two different stacking sequences obtained through electron beam evaporation where Cu is the capping layer with Cu–Sn and Cu–Zn layers being adjacent.

2. Experimental

In the current study, metallic precursors of 99.9% purity Cu, Zn and Sn are deposited using electron beam evaporation on soda lime glass substrates. CZTS films are obtained by sulphurizing the precursor film in different sulphurization environments at different ramping rates. First, soda lime glass substrates are cleaned by ultrasonication in acetone, methanol, ethanol and deionized water bath sequentially for 10 min each. The metallic layers are deposited using an electron beam evaporator with an accelerating voltage of 3.3 kV at a substrate rotation of 50 RPM without any substrate heating at a base pressure of 5×10^{-6} mbar. Cu, Zn and Sn layers of thickness 180, 160 and 230 nm respectively are deposited and the thickness and growth rate of 1 Å s^{-1} is maintained using an inbuilt quartz crystal thickness monitor. Precursor films are prepared with two stacking sequences glass/Cu (90 nm)/Zn/Sn/Cu (90 nm) (CZTC) and glass/Cu (90 nm)/Sn/Zn/Cu (90 nm) (CTZC) and the thickness of the metallic layers are chosen to have a Zn-rich, Cu-poor composition which is proven to be optimum for high efficient CZTS films. The precursor films are sulphurized in different sulphurization environments (5% $H_2S + N_2$ gas and elemental S powder with N_2 as carrier gas) at different ramping rates (1, 5 and 10°C min^{-1}) at 500°C for 1 h for conversion into CZTS films.

The phase formation on the precursors and CZTS films are analysed using X-ray diffraction (XRD) (Bruker Discover D8) with CuK_α radiation of wavelength 1.5406 Å. The effect of precursor stacking and sulphurization on the morphology and composition of the CZTS films are observed using field emission gun-scanning electron microscopy (FEG-SEM) (Carl Zeiss, Supra-S5) and energy dispersive X-ray spectroscopy (EDS) (Oxford Instrument) with an acceleration voltage of 10 kV. The phase purity of the CZTS films is studied using a Bruker Senterra Raman spectrometer with a 532 nm laser source. The optical bandgap of the CZTS films is evaluated using a Varian 5000 UV-Vis spectrophotometer.

3. Results and discussion

3.1 *Precursor film characterization*

The XRD patterns of the precursor films are shown in figure 1. Formation of Cu_6Sn_5 (JCPDS card no. 00-045-1488) and Cu_5Zn_8 (JCPDS card no. 03-065-6566) phases confirms the inter-diffusion of the adjacent layers in the precursor at room temperature itself. The presence of unreacted Sn (JCPDS card no. 86-2265) and Cu (JCPDS card no. 04-0836) is also observed.

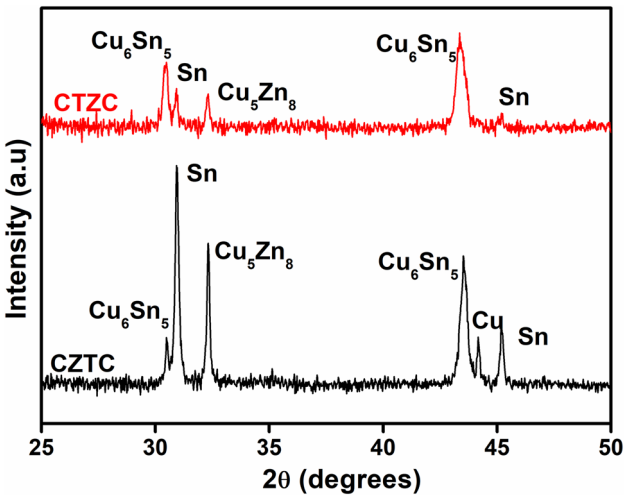

Figure 1. XRD patterns of the as-prepared precursor films.

The formation of Cu_6Sn_5 and Cu_5Zn_8 can be due to the high diffusion coefficient of Cu into Sn (2.0×10^{-11} m^2 s^{-1}) [23] and Zn into Cu (4.4×10^{-19} m^2 s^{-1}) [23]. The presence of unreacted Zn is not observed because inter-diffusion of Cu and Zn is more favourable than Cu and Sn [15].

The FEG-SEM images of the precursor films are shown in figure 2. The morphology of both the films is smooth, dense and uniform. The composition of the films is found to be Zn-rich with Zn/Sn ratio varying from 1.0 to 1.3.

3.2 *Effect of ramping rate on CZTS film formation*

For the formation of CZTS films, the as deposited precursor films are sulphurized in different sulphurization environments (5% $H_2S + N_2$ gas and elemental S powder with N_2 as carrier gas) at different ramping rates (1, 5 and 10°C min^{-1}) at 500°C for 1 h.

3.2a *XRD*: The XRD patterns of the CZTS films prepared using sulphurization in elemental S powder and H_2S environment at different ramping rates are shown in figures 3 and 4, respectively. From the XRD results, formation of CZTS (JCPDS card no. 26-0575) is confirmed.

Along with CZTS, the presence of SnS is observed only in the case of films prepared in the H_2S environment. From the intensity of the (112) peak, it can be inferred that films annealed at a low ramping rate of 1°C min^{-1} are more crystalline than higher ramping rate annealed films.

As the diffraction peaks of other secondary phases like Cu_2SnS_3 (CTS) and ZnS overlap with CZTS due to similar lattice parameters [5,17], Raman spectra of the films are essential to confirm the phase formations.

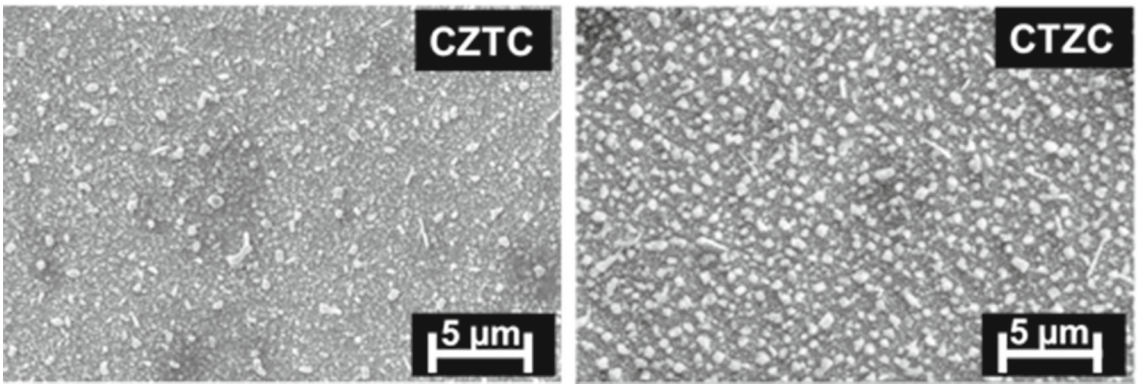

Figure 2. FEG-SEM images of the precursor films.

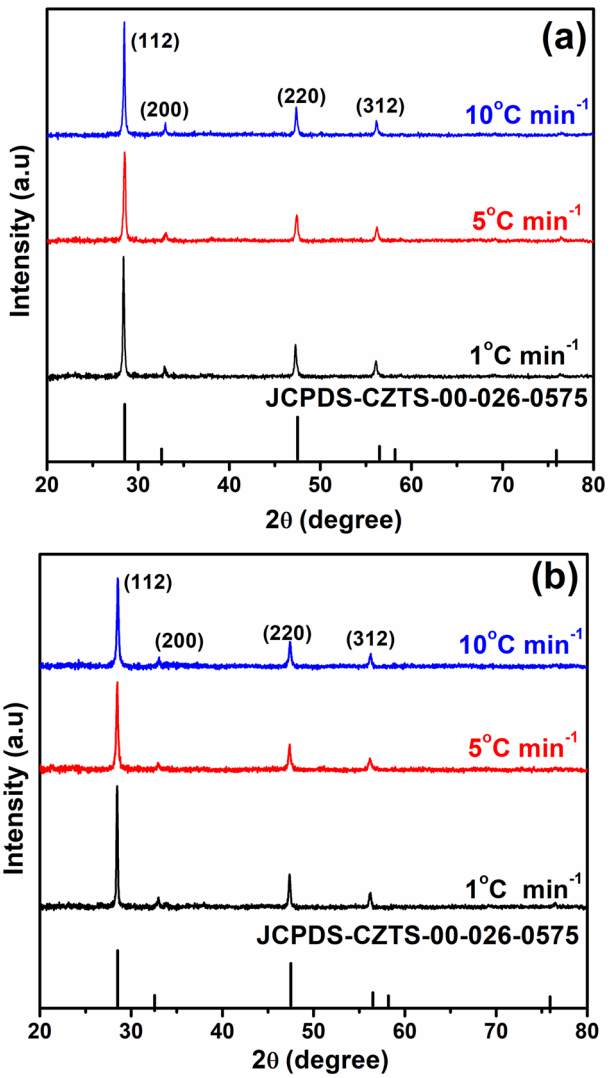

Figure 3. XRD patterns of CZTS films prepared in the elemental S powder environment using (**a**) CZTC stack and (**b**) CTZC stack.

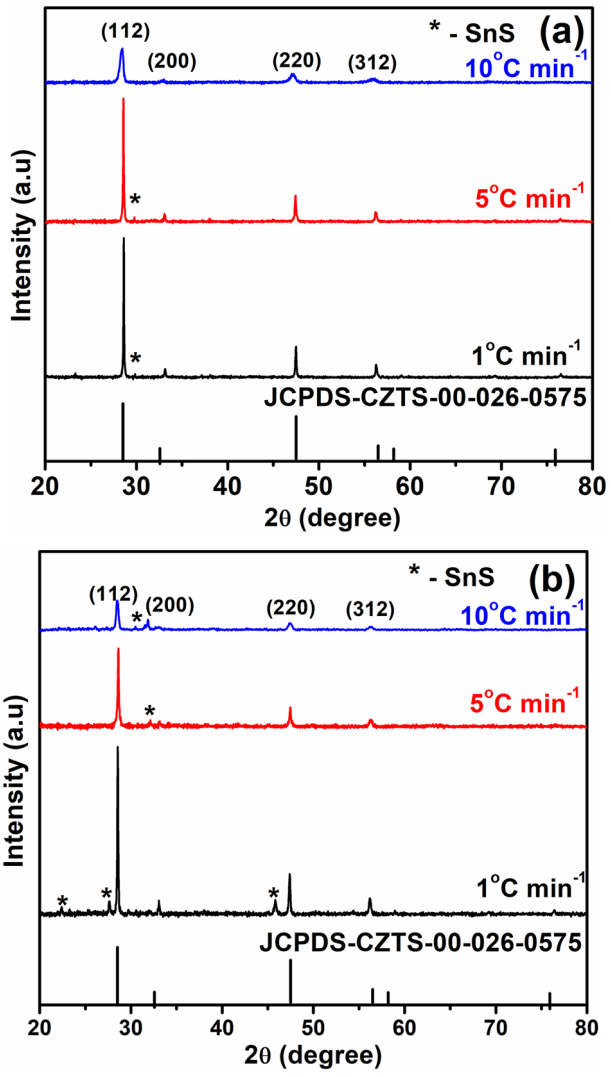

Figure 4. XRD patterns of CZTS films prepared in the 5% $H_2S + N_2$ environment using (**a**) CZTC stack and (**b**) CTZC stack.

3.2b *Raman spectroscopy*: The Raman spectra of CZTS films prepared in elemental S powder and H_2S are shown in figures 5 and 6, respectively. The presence of prominent A1 mode of CZTS (~330 cm^{-1}) [1,24] which arises due to the symmetric vibrations of anions alone in the lattice and less intense B mode (~354 cm^{-1}) which is due

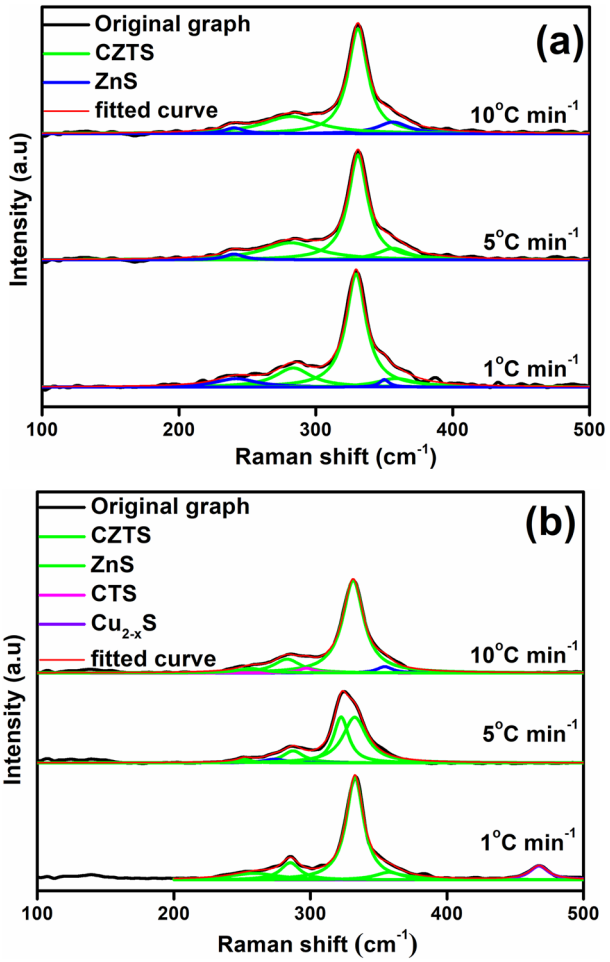

Figure 5. Raman spectra of CZTS films prepared in the elemental S powder environment using (**a**) CZTC stack and (**b**) CTZC stack.

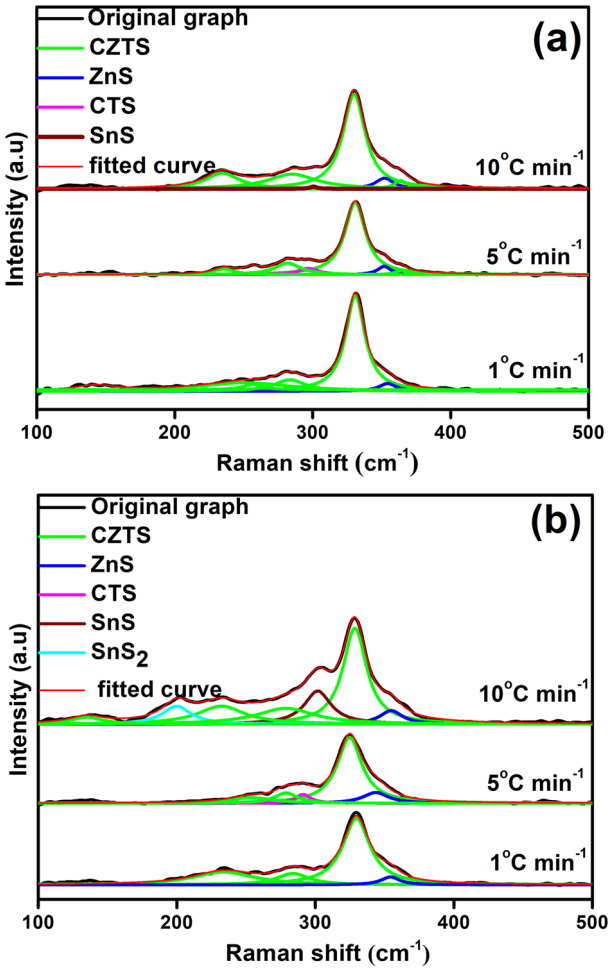

Figure 6. Raman spectra of CZTS films prepared in the 5% $H_2S + N_2$ environment using (**a**) CZTC stack and (**b**) CTZC stack.

to the movement of cations in the Z direction confirm the formation of CZTS [25]. It can be clearly seen that intensity of the A1 Raman mode of CZTS is high for films prepared with a low ramping rate and thus in agreement with the XRD results. The A1 Raman mode peaks of CZTS are not symmetric which can be due to overlapping of the CZTS peaks with secondary phase peaks. Hence, using Lorentzian function, the broad peak is deconvoluted with all possible secondary phase peaks. The black curve denotes the original spectrum, red curve is the cumulative of all the fitted curves, green curves correspond to all the CZTS modes, blue curves corresponds to ZnS modes, pink curves represent the CTS modes, violet curves represent $Cu_{2-x}S$ modes, maroon curves represent the SnS modes and cyan curves represent SnS_2 modes.

For CZTS films prepared using sulphurization of CZTC-stacked precursor film in elemental S powder, along with the CZTS peaks at 283, 329 and 359 cm^{-1} [26–28], the presence of ZnS is also detected in all the films (peaks around 242 and 350 cm^{-1}) [29,30], which can be due to the Zn-rich nature of all the films. In the case of CTZC stack, Raman results show CZTS peaks near 255, 285, 322, 331 and 358 cm^{-1} [25–28]. For the films prepared with a low ramping rate $Cu_{2-x}S$ [31] (467 cm^{-1}) phase is observed while for the films prepared at a higher ramping rate, peaks of unreacted CTS (298 cm^{-1}) [32] and ZnS (274 and 354 cm^{-1}) [28,33] are also present thus suggesting that sulphurization time of 1 h is insufficient for the formation of CZTS at a higher ramping rate.

From the Raman results of films prepared using CZTC stack in the H_2S environment, peaks around 235, 251, 284, 331 and 364 cm^{-1} [34–36] indicate the CZTS formation and peak around 352 cm^{-1} [33] is attributed to ZnS. In the films produced at a higher ramping rate, the presence of CTS (297 cm^{-1}) [32] and SnS (301 cm^{-1}) [37], clearly suggest that sulphurization time of 1 h is not enough for the formation of CZTS. For CTZC stack, it is observed that film sulphurized at a high ramping rate of 10°C min^{-1} has both SnS and SnS_2 secondary phases and thus confirms that films produced at a lower ramping rate are structurally superior with less impurity phases.

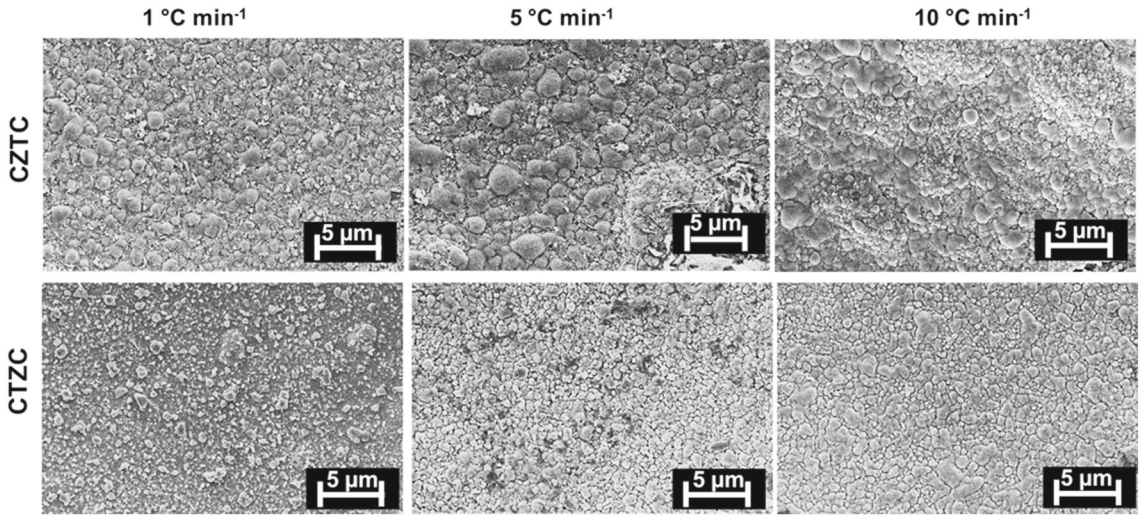

Figure 7. FEG-SEM images of CZTS films prepared using elemental S powder at different ramping rates.

Thus from the XRD and Raman results, it can be concluded that films produced through electron beam evaporation sulphurized at a low ramping rate are highly crystalline and also more suitable for solar photovoltaic applications. In the case of a higher ramping rate, coexistence of ZnS, SnS and CTS indicates that the binary sulphides do not react effectively amongst themselves.

3.3 *Effect of sulphurization environment on CZTS formation*

In the case of films annealed in the S powder environment only ZnS secondary phase is observed, while in the case of H_2S, the presence of SnS, ZnS and SnS_2 as secondary phases is observed. From this, it can be understood that formation of CZTS happens through reaction of binary sulphides which is given below [38–40]:

$$Cu_2S + ZnS + SnS_2 \leftrightharpoons Cu_2ZnSnS_4. \quad (1)$$

When the metallic films are sulphurized formation of binary sulphides Cu_2S, ZnS and SnS takes place [41]. SnS will then take up one S atom [38] and gets converted into SnS_2. As the temperature is increased further, the Cu_2S and SnS_2 react amongst each other to form Cu_2SnS_3. It reacts further with ZnS which leads to the formation of CZTS:

$$Cu_2S + SnS_2 \leftrightharpoons Cu_2SnS_3 \quad (2)$$

$$Cu_2SnS_3 + ZnS \leftrightharpoons Cu_2ZnSnS_4. \quad (3)$$

In the case of films prepared with elemental S powder, the reactions mentioned in equations (1 and 2) occur sequentially. But, in the case of H_2S, the formed SnS may not be converted efficiently into SnS_2 which may be the reason for formation of SnS impurity phases in H_2S gas case alone. It is already reported by Mangan *et al* [38] that conversion of SnS into SnS_2 requires higher energy in the case of H_2S environment which justifies our results:

$$SnS + \frac{1}{2}S_2 \rightleftharpoons SnS_2, \quad \Delta G = -27 \text{ kJ mol}^{-1} \quad (4)$$

$$SnS + H_2S \rightleftharpoons SnS_2 + H_2, \quad \Delta G = +23 \text{ kJ mol}^{-1}. \quad (5)$$

The overall free energy required for the formation of CZTS is very low in the case of elemental S powder ($\Delta G = -27$ kJ mol^{-1}) than in H_2S ($\Delta G = +28$ kJ mol^{-1}) [38]. Hence it can be concluded that CZTS phase formation is thermodynamically more effective in the case of elemental S powder.

3.3a *FEG-SEM imaging and EDS analysis*: The morphology of the films prepared with elemental S powder is shown in figure 7. It can be seen that in the case of low ramping rate, the films are having uniform moderate sized grains. But, at a higher ramping rate, the presence of large, uneven grains are observed. But, at higher ramping rate there is a minor increase in the grain size and a huge variation in the grain size and morphology are observed.

This may be due to the loss of Zn and Sn from the precursor stack, which is clearly evident from the change in the Zn/Sn ratio [42] of the film as shown in table 1. For the films prepared in the elemental S powder environment, loss of Sn from the film is observed for CZTC stack and loss of Zn is observed for CTZC stack and the amount of loss increases with increasing ramping rate [43]. This can be explained by the high volatility of Sn and Zn and thus can escape from the film before getting converted into corresponding

Table 1. Composition ratios of CZTS films prepared using elemental S powder and H_2S gas at different ramping rates.

Stack	Cu/(Zn+Sn)			Zn/Sn			(Cu+Zn+Sn)/S		
	1°C min^{-1}	5°C min^{-1}	10°C min^{-1}	1°C min^{-1}	5°C min^{-1}	10°C min^{-1}	1°C min^{-1}	5°C min^{-1}	10°C min^{-1}
CZTC sulphurized using S powder	0.83	0.84	0.77	1.02	1.06	1.19	0.98	0.98	0.99
CTZC sulphurized using S powder	1.15	1.08	1.23	1.22	1.09	0.8	1.24	1.22	1.23
CZTC sulphurized using H_2S	0.75	0.79	0.79	1.28	1.14	0.93	0.98	0.96	1.26
CTZC sulphurized using H_2S	0.86	1.31	1.71	1.02	1.03	0.67	0.94	1.15	1.30
Precursor CZTC		0.9			1.01			—	
Precursor CTZC		1.24			1.36			—	

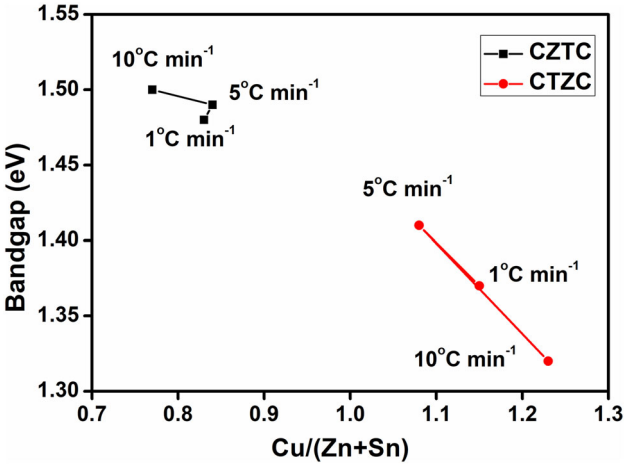

Figure 8. Optical bandgap of CZTS films prepared using elemental S powder at different ramping rates.

binary sulphides [8]. In the case of films annealed in the H_2S environment, loss of Sn is observed in the case of CZTC stack, while loss of Zn is observed in the case of CTZC stack.

The precursor stacking plays a prominent role in determining the loss of elemental Sn and Zn from the stack. In the case of CZTC stack, where Sn is at the top portion, loss of Sn dominates while for the CTZC stack, loss of Zn dominates.

3.3b *UV–Vis spectroscopy*: The optical bandgap of the CZTS films are found using Tauc plot where $(\alpha h\upsilon)^2$ *vs.* photon energy plot is extrapolated according to the relationship $(\alpha h\upsilon) = A(h\upsilon - E_g)^n$ and $\alpha = 2.303A/t$ where α denotes the linear absorption coefficient, A is the absorbance of the film, t is the film thickness, E_g represents optical band gap of material and $n = 1/2$ for direct allowed transition [5,24]. The composition of the films have a huge impact on the bandgap of the CZTS [6] and hence the optical bandgap of the films prepared with elemental S powder is compared with their Cu/(Zn+Sn) ratio and the values are shown in figure 8.

The bandgap of the films is found to be increasing with decreasing Cu/(Zn+Sn) ratio which is in agreement with the earlier results [44]. This can be due to the increase in the formation of V_{cu-} (Cu-vacancy) and decrease in the formation of detrimental $[2Cu_{Zn} + Sn_{Zn}]$ defect clusters at low Cu/(Zn+Sn) concentrations [6]. The bandgap of the best film with 1.48 eV is fabricated by the sulphurization of CZTC stack in the presence of elemental S powder at a low ramping rate of 1°C min^{-1}.

4. Conclusions

In the present work, CZTS films are prepared from electron beam evaporation of two different precursors with stacking sequences (glass/Cu/Zn/Sn/Cu and glass/Cu/Sn/Zn/Cu). It is

found that sulphurization environment and ramping rate have a crucial impact on the formation of CZTS films. It is concluded that sulphurization in elemental S powder at a low ramping rate is found to be more effective in CZTS formation when compared to the H_2S environment. A Zn-rich, Cu-poor CZTS film with a bandgap of 1.48 eV is fabricated using sulphurization of glass/Cu/Zn/Sn/Cu stacking sequence in elemental S powder at a low ramping rate of $1^{\circ}C\ min^{-1}$.

References

[1] Altamura G and Vidal J 2016 *Chem. Mater.* **28** 3540
[2] Ito K 2014 *Copper zinc tin sulfide-based thin-film solar cells* (UK: John Wiley & Sons)
[3] Kang 2016 Reported at PVSEC-36 by a research team led at DGIST in South Korea. A 0.181 cm^2 solar cell was certified at 13.80% by KIER
[4] Wallace S K, Mitzi D B and Walsh A 2017 *ACS Energy Lett.* **2** 776
[5] Chaudhari S, Kannan P K and Dey S R 2016 *Thin Solid Films* **612** 456
[6] Chen S, Walsh A, Gong X G and Wei S H 2013 *Adv. Mater.* **25** 1522
[7] Katagiri H, Yokota T, Sasaguchi N, Ohashi J, Hando S and Hoshino S 1997 *Sol. Energy Mater. Sol. Cells* **49** 407
[8] Johnson M C, Wrasman C, Zhang X, Manno M, Leighton C and Aydil E S 2015 *Chem. Mater.* **27** 2507
[9] Chaudhari S, Kannan P K and Dey S R 2016 *Conf. Rec. IEEE Photovolt. Spec. Conf.* p. 1429
[10] Chaudhari S, Kannan P K and Dey S R 2017 *Thin Solid Films* **636** 144
[11] Todorov T K, Tang J, Bag S, Gunawan O, Gokmen T, Zhu Y *et al* 2013 *Adv. Energy Mater.* **3** 1
[12] Scragg J J, Dale P J and Peter L M 2009 *Thin Solid Films* **517** 2481
[13] Kim J and Yoo H 2011 *Sol. Energy Mater. Sol. Cells* **95** 239
[14] Araki H, Mikaduki A, Kubo Y, Sato T, Jimbo K, Maw W S *et al* 2008 *Thin Solid Films* **517** 1457
[15] Su C-Y, Yen Chiu C and Ting J-M 2015 *Sci. Rep.* **5** 9291
[16] Katagiri H, Saitoh K, Washio T, Shinohara H, Kurumadani T and Miyajima S 2001 *Sol. Energy Mater. Sol. Cells* **65** 141
[17] Shin S W, Pawar S M, Park C Y, Yun J H, Moon J H, Kim J H *et al* 2011 *Sol. Energy Mater. Sol. Cells* **95** 3202
[18] Wang W, Winkler M T, Gunawan O, Gokmen T, Todorov T K, Zhu Y *et al* 2014 *Adv. Energy Mater.* **4** 1
[19] Collord A D and Hillhouse H W 2015 *Chem. Mater.* **27** 1855
[20] Thota N, Gurubhaskar M, Sunil M A, Prathap P, Subbaiah Y P V and Tiwari A 2017 *Appl. Surf. Sci.* **396** 644
[21] Olgar M A, Klaer J, Mainz R, Levcenco S, Just J, Bacaksiz E *et al* 2016 *Thin Solid Films* **615** 402
[22] Khalil M I, Bernasconi R, Ieffa S, Lucotti A, Le Donne A, Binetti S *et al* 2015 *ECS Trans.* **64** 33
[23] Scragg J J 2011 *Copper zinc tin sulfide thin films for photovoltaics – synthesis and characterisation by electrochemical methods* (Berlin: Springer)
[24] Chaudhari S, Kannan P K and Dey S R 2017 *Thin Solid Films* **636** 144
[25] Dumcenco D and Huang Y-S 2013 *Opt. Mater. (Amst).* **35** 419
[26] Rajesh G, Muthukumarasamy N, Subramaniam E P, Agilan S and Velauthapillai D 2013 *J. Sol-Gel Sci. Technol.* **66** 288
[27] Thankalekshmi R R and Rastogi A C 2015 *42nd Photovolt. Spec. Conf. PVSC 2015*
[28] Patel K, Shah D V and Kheraj V 2015 *J. Alloys Compd.* **622** 942
[29] Cheng Y C, Jin C Q, Gao F, Wu X L, Zhong W, Li S H *et al* 2009 *J. Appl. Phys.* **106** 1
[30] Jiang F, Shen H, Wang W and Zhang L 2011 *Appl. Phys. Express* **4** 074101
[31] Pani B, Singh R K and Singh U P 2015 *J. Alloys Compd.* **648** 332
[32] Guan H, Shen H, Gao C and He X 2013 *J. Mater. Sci. Mater. Electron.* **24** 1490
[33] Xia D, Lei P, Zheng Y and Zhou B 2015 *J. Mater. Sci. Mater. Electron.* **26** 5426
[34] Mkawi E M, Ibrahim K, Ali M K M and Mohamed A S 2013 *Int. J. Electrochem. Sci.* **8** 359
[35] Caballero R, Garcia-Llamas E, Merino J M, León M, Babichuk I, Dzhagan V *et al* 2014 *Acta Mater.* **65** 412
[36] Grossberg M, Krustok J, Raudoja J, Timmo K, Altosaar M and Raadik T 2011 *Thin Solid Films* **519** 7403
[37] Alzaidy G A, Huang C and Hewak D W 2015 *11th Photovolt. Sci. Appl. Technol. Conf. (PVSAT-11)*, Leeds, GB
[38] Mangan T C, McCandless B E, Dobson K D and Birkmire R W 2015 *J. Appl. Phys.* **118** 65303
[39] Ahmad R, Brandl M, Distaso M, Herre P, Spiecker E, Hock R *et al* 2015 *CrystEngComm* **17** 6972
[40] Mainz R, Walker B C, Schmidt S S, Zander O, Weber A, Rodriguez-Alvarez H *et al* 2013 *Phys. Chem. Chem. Phys.* **15** 18281
[41] Hock R, Kirbs A, Schurr R, Voß T, Jost S, Weber A *et al* 2009 *Thin Solid Films* **517** 2465
[42] Unveroglu B and Zangari G 2016 *Electrochim. Acta* **219** 664
[43] Feng Y, Yu B, Cheng G, Lau T, Li Z, Yin L *et al* 2015 *J. Mater. Chem. C* **3** 9650
[44] Suresh Babu G, Kishore Kumar Y B, Uday Bhaskar P and Raja Vanjari S 2010 *Sol. Energy Mater. Sol. Cells* **94** 221